N89-12897

MEASUREMENT OF AIRFOIL HEAT TRANSFER COEFFICIENTS ON A TURBINE STAGE*

Robert P. Dring
Michael F. Blair
H. David Joslyn

United Technologies Research Center
East Hartford, Connecticut 06108

INTRODUCTION

The Primary basis for heat transfer analysis of turbine airfoils is experimental data obtained in linear cascades. These data have been very valuable in identifying the major heat transfer and fluid flow features of a turbine airfoil. The question of major interest is how well all of these data translate to the rotating turbine stage. It is known from the work of Lokay and Trushin (Ref. 1) that average heat transfer coefficients on the rotor may be as much as 40 percent above the values measured on the same blades non-rotating. Recent work by Dunn and Holt (Ref. 2) supports the conclusion of Ref. 1. What is lacking is a set of data from a rotating system which is of sufficient detail as to make careful local comparisons between static cascade and rotor blade heat transfer. In addition, data is needed in a rotating system in which there is sufficient documentation of the flow field to support the computer analyses being developed today. Other important questions include the impact of both random and periodic unsteadiness on both the rotor and stator airfoil heat transfer. The random unsteadiness arises from stage inlet turbulence and wake generated turbulence and the periodic unsteadiness arises from blade passing effects. A final question is the influence, if any, of the first stator row and first stator inlet turbulence on the heat transfer of the second stator row after the flow has been passed through the rotor.

OBJECTIVES

The first program objective is to obtain a detailed set of heat transfer coefficients along the midspan of a stator and a rotor in a rotating turbine stage. These data are to be such that the rotor data can be compared directly with data taken in a static cascade. The data are to be compared to some standard analysis of blade boundary layer heat transfer which is in use today. In addition to providing this all-important comparison between rotating and stationary data, this experiment should provide important insight to the more elaborate full three-dimensional programs being proposed for future research. A second program objective is

*Work done under NASA Contract NAS 3-2317.

to obtain a detailed set of heat transfer coefficients along the midspan of a stator located in the wake of an upstream turbine stage. Particular focus here is on the relative circumferential location of the first and second stators. Both program objectives will be carried out at two levels of inlet turbulence. The low level will be on the order of 1 percent while the high level will be on the order of 10 percent which is more typical of combustor exit turbulence intensity. The final program objective is to improve the anlytical capability to predict the experimental data.

DESCRIPTION OF EXPERIMENTAL EQUIPMENT AND TEST CONDITIONS

The experimental portion of this study was conducted in large-scale (aproximately 5x engine), ambient temperature, rotating turbine model configured in both single stage and stage-and-a-half arrangements. A cross-sectional diagram of the turbine model in the stage-and-a-half configuration is presented in Figure 1. Heat transfer measurements were obtained using low-conductivity airfoils with miniature thermocoulpes welded to a thin, electrically heated surface skin. Heat transfer data were acquired for various combinations of low or high inlet turbulence intensity, flow coefficient, first-stator/rotor axial spacing, Reynolds number and relative circumferential position of the first and second stators. High levels of inlet turbulence were generated using a coarse biplane grid located 2 1/2 axial chords upstream of the stator leading edge plane(see Figure 1). Aerodynamic measurements obtained as part of the program include distributions of the mean and fluctuating velocities at the turbine inlet and, for each airfoil row, midspan airfoil surface pressures and circumferential distributions of the downstream steady state pressure and fluctuating velocities.

Time-mean velocity distributions at the inlet to the turbine model, obtained both with and without the turbulence grid installed, are presented in Figures 2a and 2b. These figures indicate that, both with and without the grid, the spanwise variations of mean velocity at each pitch location were quite small and that the pitchwise velocity variations were in excellent agreement with a potential flow prediction. The distributions of streamwise turbulence intensity measured with and without the grid are presented in Figure 3. As shown in Figure 3a, with the grid out the midspan region turbulence intensity was slightly greater than 1/2% with much higher levels in the endwall boundary layers. With the grid in, as shown in Figure 3b, the midspan turbulence intensity averaged 9.8%. Spectral measurements of the grid generated turbulence indicated that it was in excellent agreement with the von Karman isotropic spectrum.

RESULTS

Distributions of heat transfer along the various airfoil surfaces are presented as Stanton numbers based on exit conditions vs dimensionless

surface distance. Included in each figure are the specific flow coefficient and axial spacing for the data set and a note indicating whether the turbulence grid was IN or OUT.

Midspan first stator heat transfer distribution data obtained for the single-stage configuration for three Reynolds numbers and low inlet turbulence are presented in Figure 4. The experimental data are compared to distributions predicted by the UTRC two-dimensional finite difference boundary layer code (ABLE, Ref.3). Predictions for both fully laminar (L) and fully turbulent (T) flow (Cebeci-Smith, Ref.4) are included. On the pressure surface, agreement with the fully laminar prediction was excellent for all three Reynolds numbers. Evidence of possible boundary layer transition near the pressure surface trailing edge progressively decreased with decreasing Reynolds number. On the suction surface the agreement between the laminar prediction and the upstream half of the data was also excellent in all cases. A careful examination of the data near S/Bx=1 indicates that transition moved progressively, albeit slightly, downstream as Reynolds number decreased. Finally for S/Bx>1 both the highest andlowest Re data agreed very well with the two-dimensional fully turbulent prediction. For $Re=52x10^4$ an anamolous discrepancy of about 10% between theory and data resulted for this region. One possible explanation for this shift is that an undetected shift in model heater power occured during the process of automatic data acquisition.

The primary conclusion reached from Fig. 4 is that the facility, turbine model and instrumentation system all behaved as expected. As the Reynolds number changed for this relatively idealized first stator flow the data and two-dimensioinal theory remained in excellent agreement.

Rotor heat transfer distributions for the single-stage configuration are presented in Figure 5 for three Reynolds numbers. Again each data set is shown compared with the two-dimensional fully turbulent prediction for that particular Reynolds number. On the suction surface there was an increasingly significant, both in size and heat transfer level, transitional region as the Reynolds number dropped. For all cases, however, the heat transfer data agreed reasonably well with the two-dimensional, fully turbulent boundary layer prediction in the trailing edge region.

The rotor pressure surface heat transfer distributions shown in Figures 5 reveal a dependence on the Reynolds number. At the lightest Reynolds number the pressure surface heat transfer is significantly higher (50 to 80% higher) than the fully turbulent prediction. As the Reynolds number drops the data approach their respective predictions. Elevated levels of pressure surface heat transfer were observed for numerous airfoil-flow condition combinations in this investigation. Discussion of the phenomenon will follow as more examples are presented.

The effects on the first stage heat transfer distributions produced by raising the inlet turbulence intensity are shown in Figure 6. The impact of the high inlet turbulence on the first stator distribution was dramatic

with significant increases of heat transfer on the leading edge and along both suction and pressure surfaces. On the suction surface the increased turbulence moved the location of transition well upstream from S/Bx=1.0 to about S/Bx=0.3. For this high level of turbulence, then, transition occured in a region of accelerating flow instead of near the minimum pressure point. Another effect of the turbulence on the suction surface distribution was to produce considerably enhanced heat transfer in the fully turbulent region of the flow. The effect of the higher turbulence level was also very evident along the stator pressure surface. For the low turbulence case the heat transfer was essentially laminar while with high turbulence the measured heat transfer was as much as 60% greater than the two-dimensional fully turbulent prediction. The data of Figure 6a constitute another example of an airfoil-flow condition combination for which the measured/pressure surface heat transfer far exceeded fully turbulent levels.

On the rotor, Figure 6b, the effects produced by increasing the inlet turbulence were much less dramatic than for the first stator. A much smaller change to the heat transfer resulted for the rotor because even the baseline (low inlet turbulence) rotor flow is highly disturbed by the first stator wakes. The incremental change in the distrubance level produced by installing the grid was much less for the rotor than for the first stator. On the rotor suction surface, transition appears to have moved upstream to S/Bx$\sim$0.2 with the increased turbulence level. Changes downstream of transition in the fully turbulent region were negligible. The only region of the rotor pressure surface which showed any effects from the increased turbulence was from $-0.5<S/Bx<0$.

Figure 7 displays the impact of Reynolds number on the first stator heat transfer distributions with high inlet turbulence. On the suction surface Figure 7 shows an orderly, progressive downstream movement of the transition zone with decreasing Reynolds number. As the Reynolds number decreased the length of the near-laminar heat transfer zone increased and the length of the fully turbulent zone contracted. On the pressure surface the data show that for the highest Reynolds number the measured heat transfer greatly exceeded the turbulent prediction while for $Re < 4x10^5$ there was near agreement between theory and experiment.

A number of examples have been presented in which pressure surface heat transfer rates significantly exceeded two-dimensional, fully turbulent predictions. These results indicate that there can be an interaction between the effects of concave surface curvature, Reynolds number and the level of free-stream disturbance that may produce significant heat transfer enhancement. One possibility is that for certain critical combinations of surface curvature, Re_θ, acceleration and free-stream disturbance level, important Goertler vortex systems are produced in the boundary layer.

Rotor heat transfer distributions obtained for an extremely wide range of test flow coefficients are presented in Figure 8. These results reflect operation at severe off-design conditions and are included to demonstrate the impact on heat transfer for such extreme excursions. On the suction surface, for S/Bx<0.7, the local Stanton numbers decreased with Cx/U until

they approached laminar heat transfer rates. On the pressure surface there was a continuous, systematic increase in Stanton numbers through the entire range of test flow coefficients. The appearance of the distributions suggests that for Cx/U <0.5 the flow probably separated from the pressure surface. At these extreme negative incidence values the heat transfer was evidently dominated by a large, possible unsteady, pressure surface separation bubble.

Heat transfer distributions measured on the second stator are presented in Figure 9. These data were obtained for five relative circumferential positions of the first and second stators with and without the grid.

Probably the most striking feature of the second stator heat transfer distributions, both for the grid-in and grid-out are the very high values of Stanton number relative to the two-dimensional turbulent boundary layer prediction. On the pressure surface the heat transfer data are 50-100% above the prediction, a result which is in general agreement with most of the first stator and rotor pressure surface measurements. On the suction surface, however, the second vane heat transfer is entirely different from the first stage results. Not only are the suction surface heat transfer data well in excess of the two-dimensional prediction but the data and theory are diverging with increasing S. It appears that by the second stator the flow field has become so contaminated by secondary flow that a two-dimensional model is inappropriate. The effects associated with stator 1/stator 2 relative location appear to have been minor.

A detailed distribution of the heat transfer measured in the leading edge region of the first stator with the grid in is given in Figure 10. For these figures the heat transfer data are presented in the form of the Froessling number $Nu/\sqrt{Re_D}$ where the Reynolds number is based on the diameter of the leading edge. Locations are given as S/R_N, the surface distance divided by the nose radius. Note that, unlike a cylinder in crossflow, the theoretical heat transfer distribution is not symmetrical about the stagnation point. In addition, since the acceleration is very much stronger in the direction of the suction surface, the maximum predicted heat transfer rate is not at the stagnation point. The results of Figure 10 are quite surprising in that the heat transfer measured for the highly turbulent test flow was only about 20% greater than the predicted laminar levels. Data taken in a number of studies of cylinders in crossflows have indicated that freestream turbulence has a very strong effect on the stagnation region heat transfer (see Lowery and Vachon, Ref.5). It may be that the effects of turbulence are much larger for free cylinders than for airfoil leading edges.

A comparison of the heat transfer distribution measured in a previous investigation in a cascade (Ref.6) with the data obtained on the rotor of the present study is presented in Figure 11. These two data sets were obtained at somewhat different Reynolds numbers so predicted heat transfer distributions are given for both conditions. An examination of Figure 11 indicates that, on the suction surface, transition was somewhat earlier for the rotating case than for the blade cascade. This result is not

surprising as the disturbance level for the rotating blade was considerably higher than the 1% turbulence level at the entrance plane of the cascade. When allowance is made for the effect of Reynolds number, the post-transitional (S/Bx > 0.8) results for the rotating and cascade tests were practically identical. There was, however, a significant difference between the heat transfer distributions measured on the pressure surface with the cascade data falling well below the set from the rotating blade. This provides an additional piece of evidence which indicates that strong enhancement of fully turbulent, concave surface heat transfer may only occur for high levels of free-stream disturbance. Whatever the cause, the major difference between the rotating and non-rotating airfoil midspan heat transfer distributions was the considerably higher levels on the pressure surface of the rotating airfoil.

The heat transfer data measured in the leading edge region of the cascade airfoils are presented in Figure 12. Included in Figure 12 are the predicted laminar distributions for this airfoil as well as the comparable leading edge data from the rotating cases. Because of the instrumentaiton techniques employed the experimental uncertainty is considerably greater for the cascade leading edge data than for the rotating airfoil. Despite the data scatter associated with the cascade model it is still clear that the stagnation region heat transfer was reasonably well predicted by the laminar model. There was no evidence that the moderate (1%) free-stream turbulence in the cascade tunnel substantially enhanced the heat transfer in the leading edge region of the airfoil.

REFERENCES

1. Lokay, V. I., and Trushin, V. A.: Heat Transfer from the Gas and Flow-Passage Elements of a Rotating Gas Turbine. Heat Transfer-Soviet Research, Vol. 2., No. 4, July, 1970.

2. Dunn, M. G., and Holt, J. L.: The Turbine Stage Heat Flux Measurements. Paper No. 82-1289, AIAA/ASME 18th Joint Propulsion Conference, 21-23, June, 1982, Cleveland, Ohio.

3. Carter, J. E., D. E. Edwards and M. J. Werle: Coordinate Transformation for Laminar and Turbulent Boundary Layers, AIAA Journal, Vol. 20, No. 2, February 1982, pp. 282-284.

4. Cebeci T. and A. M. O. Smith: Analysis of Turbulent Boundary Layers, Academic Press, 1974.

5. Lowery, G. W. and Vachon, R. I.: The Effect of Turbulence on Heat Transfer From Heated Cylinders, IJHMT, Vol. 18, 1975, pp.1229-1242.

6. Graziani, R. A., M. F. Blair, J. R. Taylor and R. E. Mayle: An Experimental Study of Endwall and Airfoil Surface Heat Transfer in a Large Scale Turbine Blade Cascade, ASME Journal of Eng. for Power, Vol. 102, April 1980, pp. 257-267.

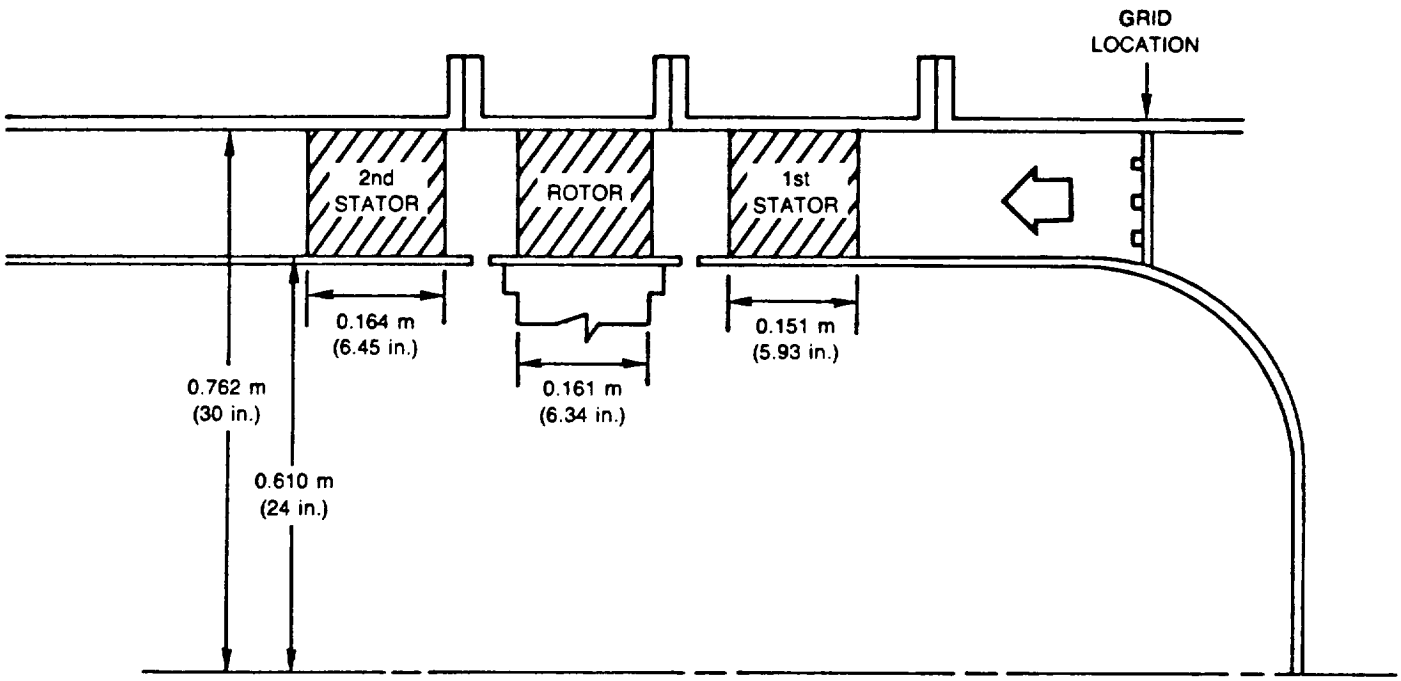

Figure 1 United Technologies Research Center Large Scale Rotating Rig.

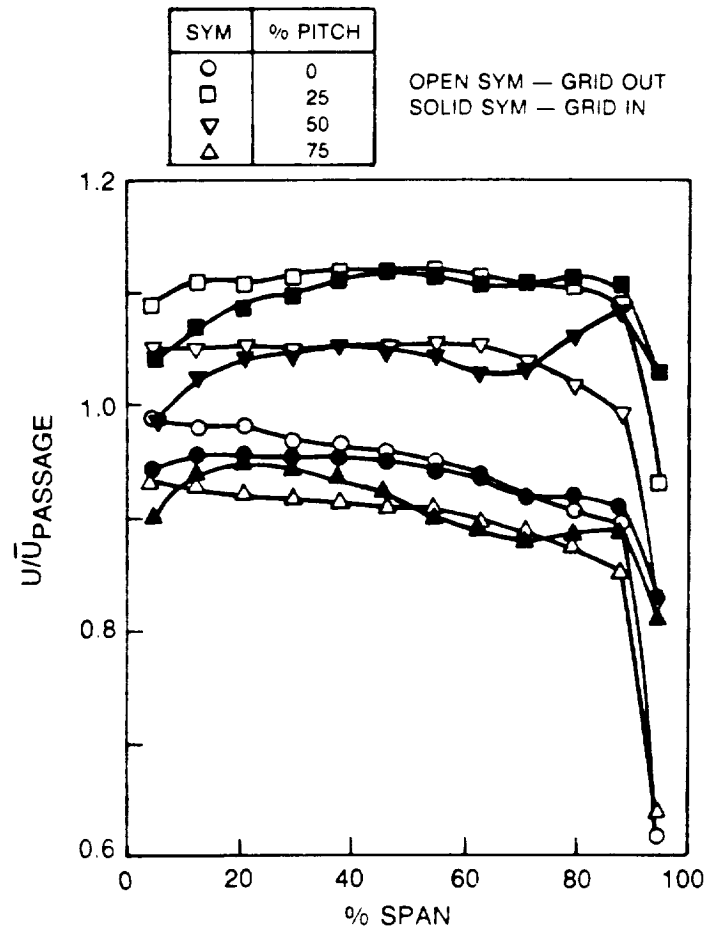

a) SPANWISE DISTRIBUTIONS OF THE TEMPORALLY AVERAGED STREAMWISE VELOCITY AT VARIOUS PITCH LOCATIONS

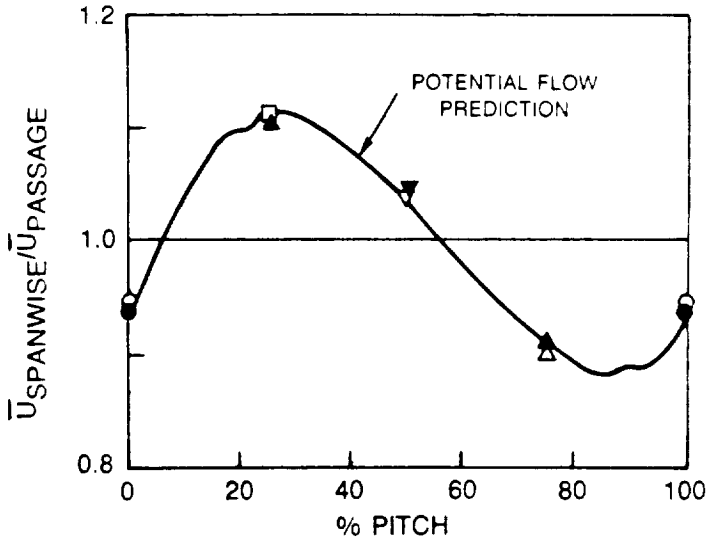

b) SPANWISE AVERAGED STREAMWISE VELOCITIES

Figure 2 Distributions of the Mean Velocity at X=-3.4cm (-23% Bx).

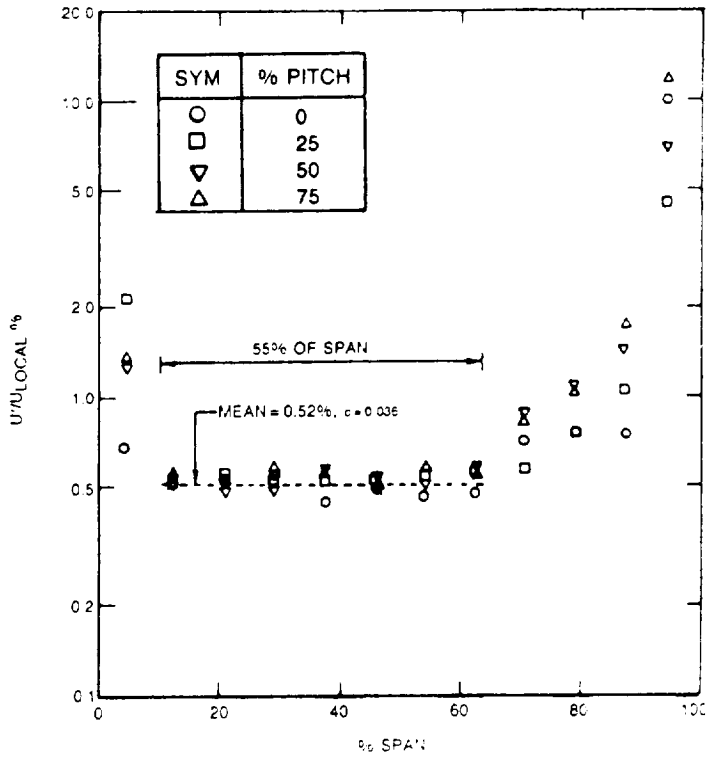

a) GRID OUT

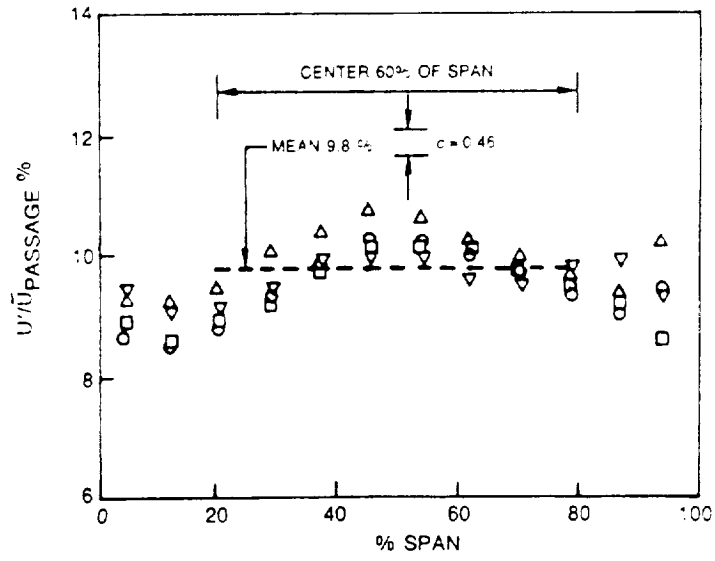

b) GRID IN

Figure 3 RMS Level of the Streamwise Component of Turbulence at X=-3.4cm (-23% Bx) at Various Pitch Locations.

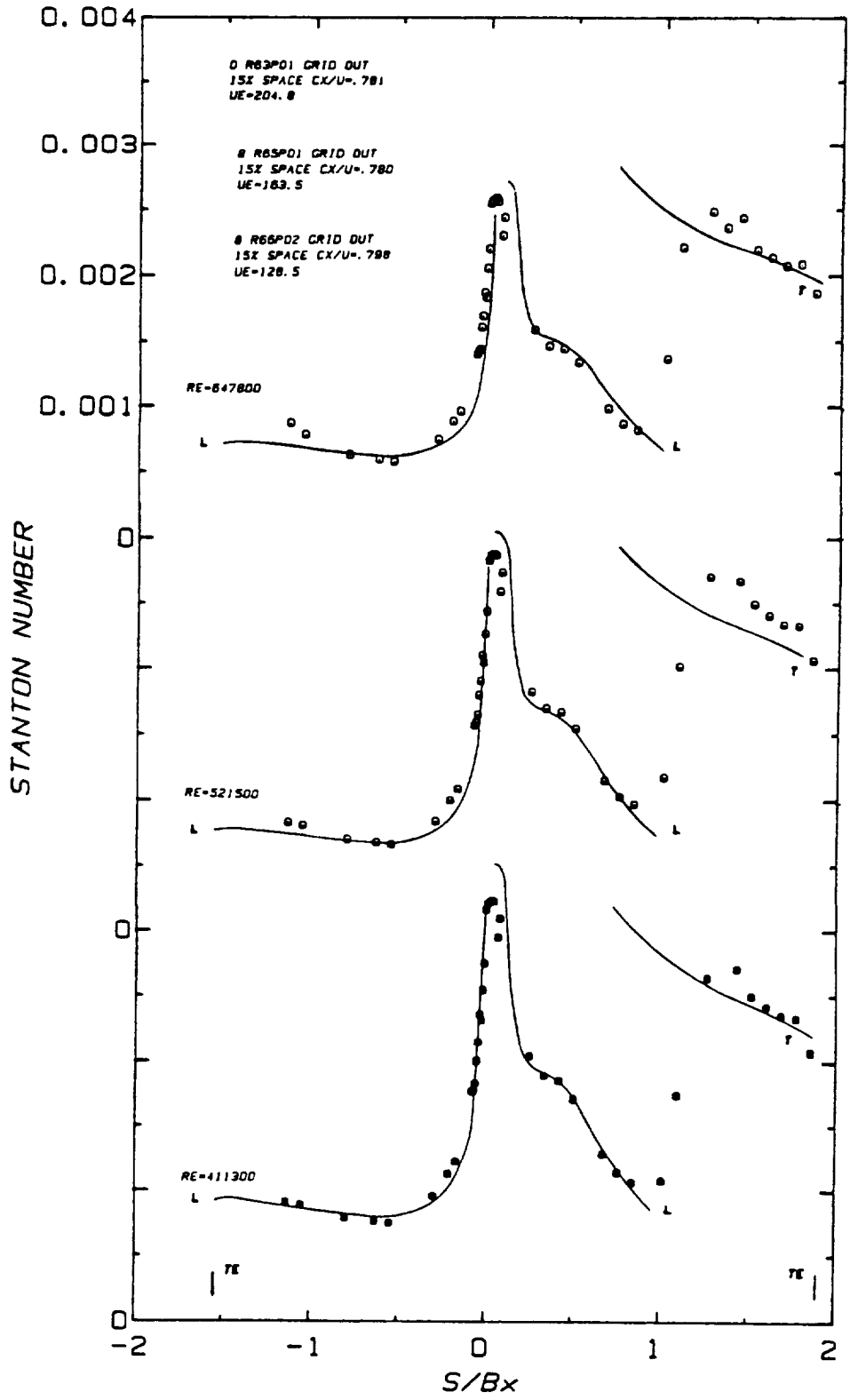

Figure 4 Effect of Reynolds Number on the Stator Heat Transfer, Grid Out.

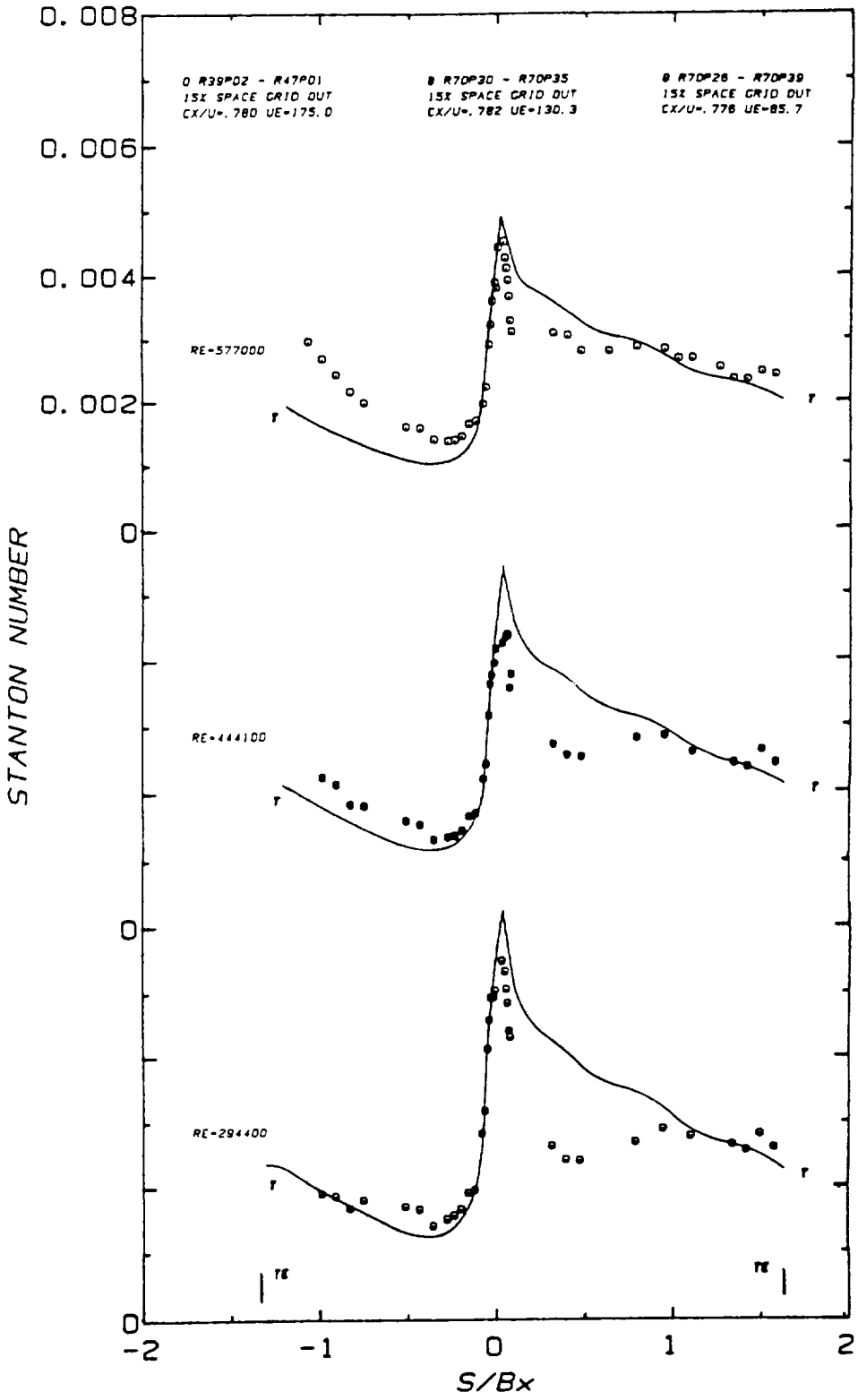

Figure 5 Effect of Reynolds Number on the Rotor Heat Transfer, Design Flow Coefficient, Grid Out.

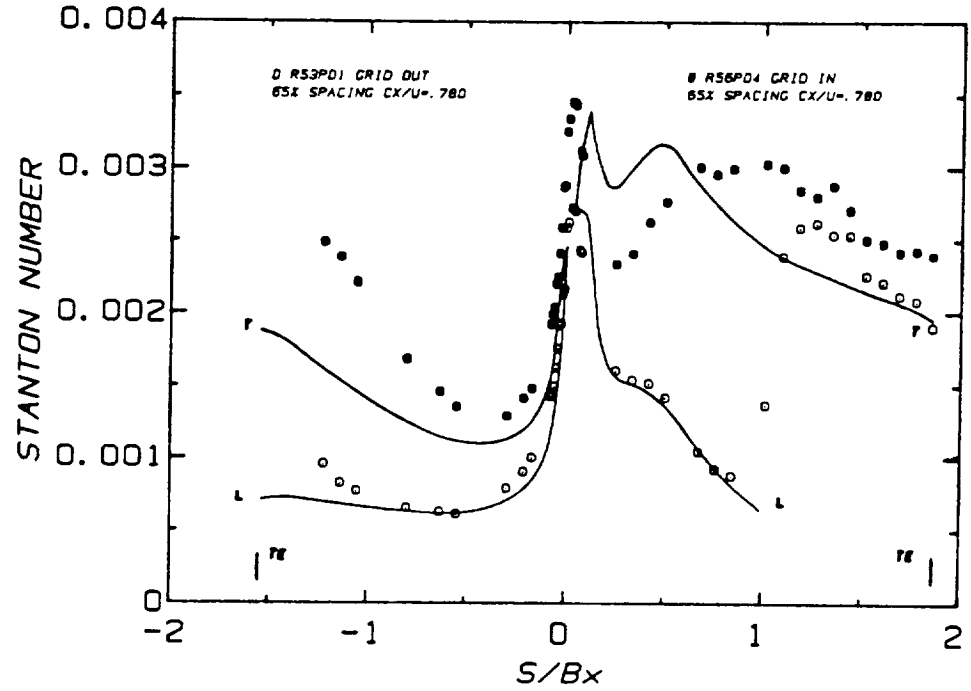

a) SINGLE-STAGE STATOR

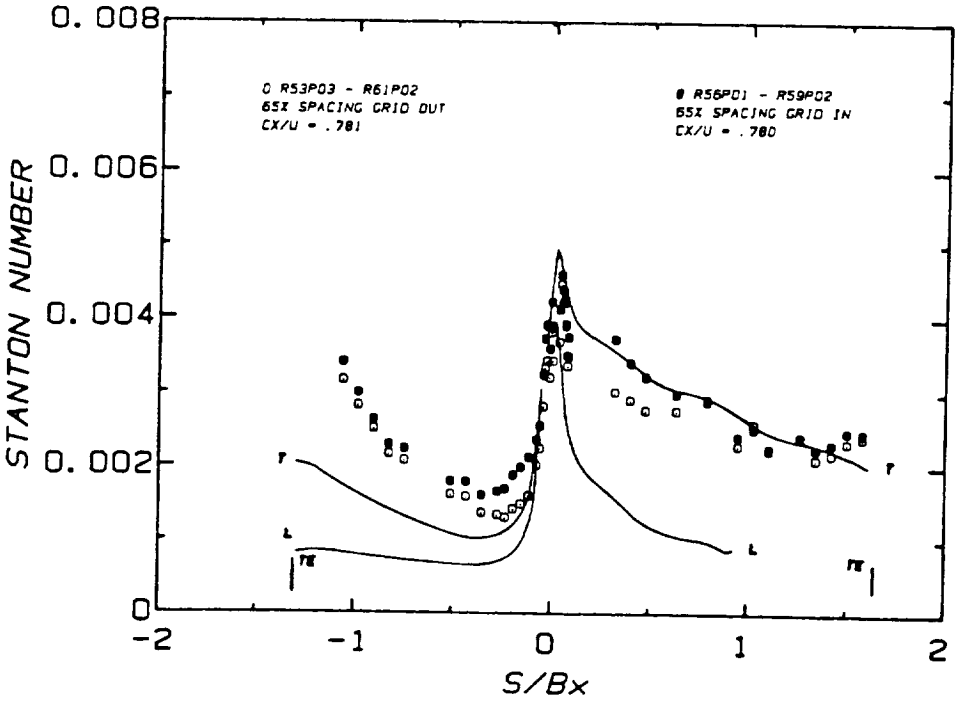

b) SINGLE-STAGE ROTOR

Figure 6 Effect of Free-Stream Turbulence on the Stator and Rotor Heat Transfer for the Single-Stage Configuration and Design Flow Coefficient.

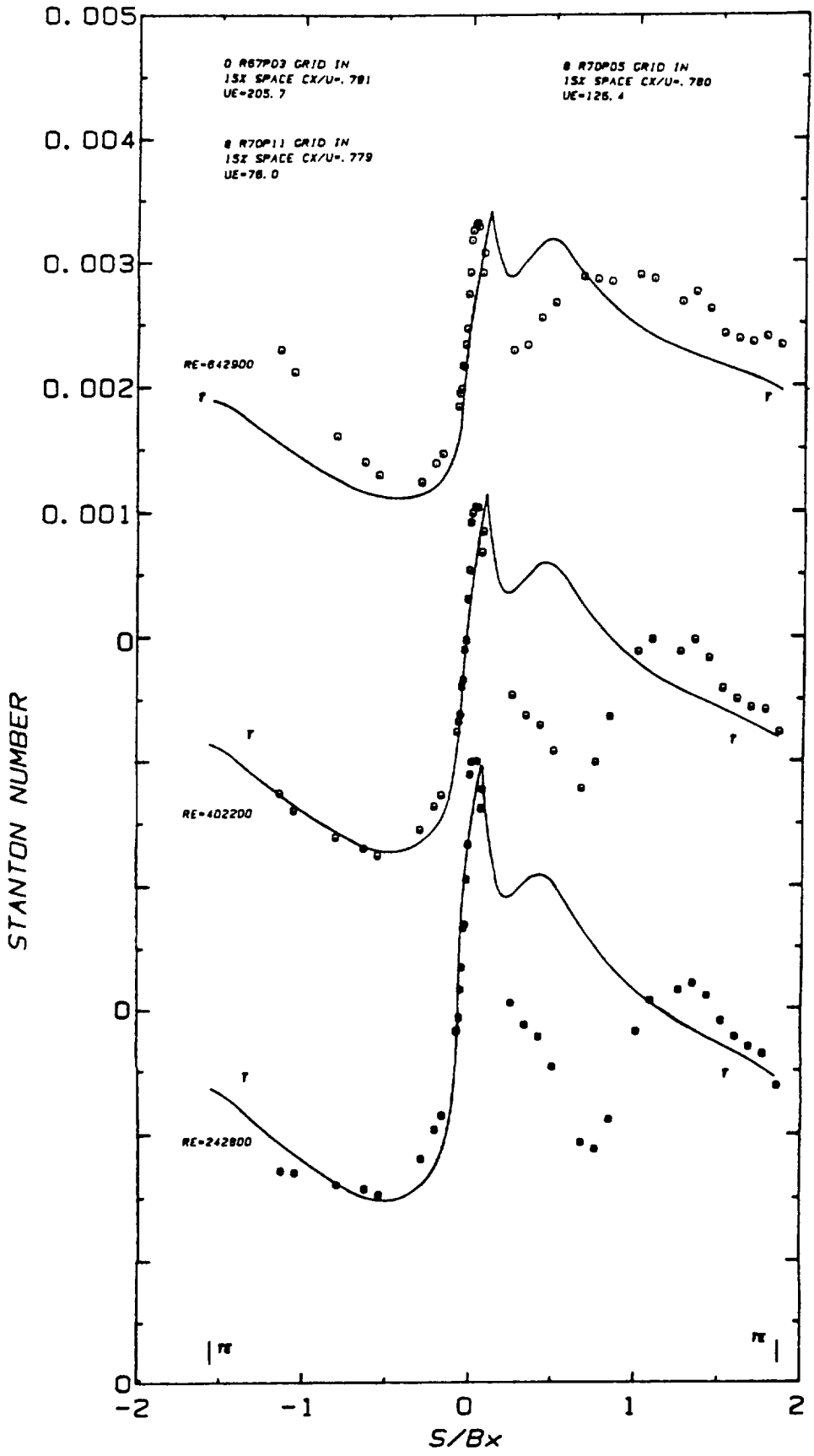

Figure 7 Effect of Reynolds Number on the Stator Heat Transfer, Grid In.

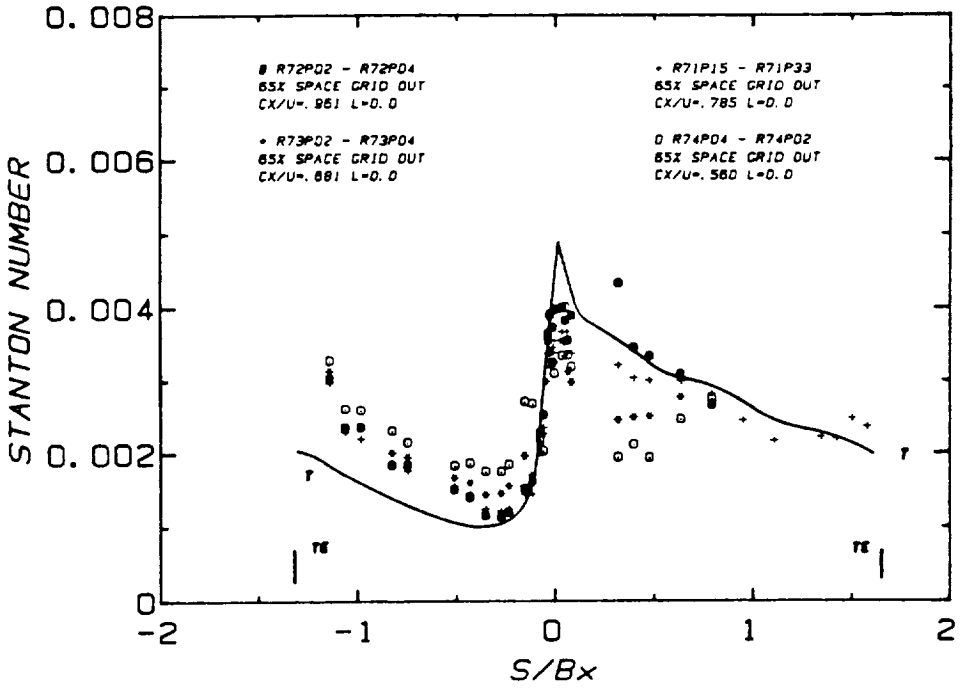

a) Cx/U = 0.96, 0.79, 0.68 and 0.56

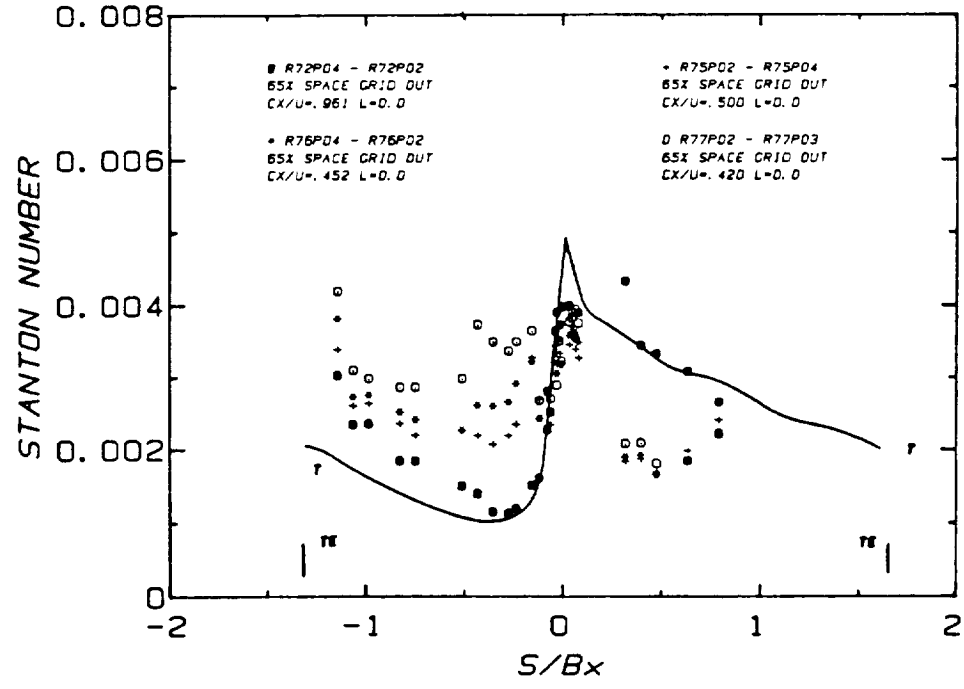

b) Cx/U = 0.96, 0.50, 0.45 and 0.42

Figure 8 Effect of Extreme Variation of the Flow Coefficient on the Rotor Heat Transfer Distribution, 1-1/2 Stage Configuration, Grid Out.

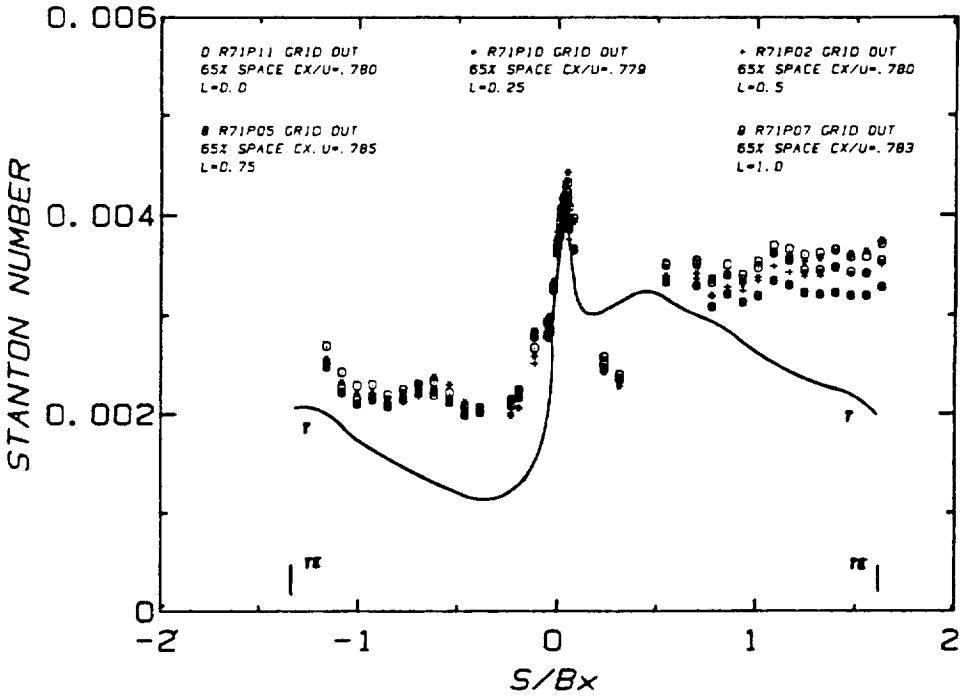

a) GRID OUT

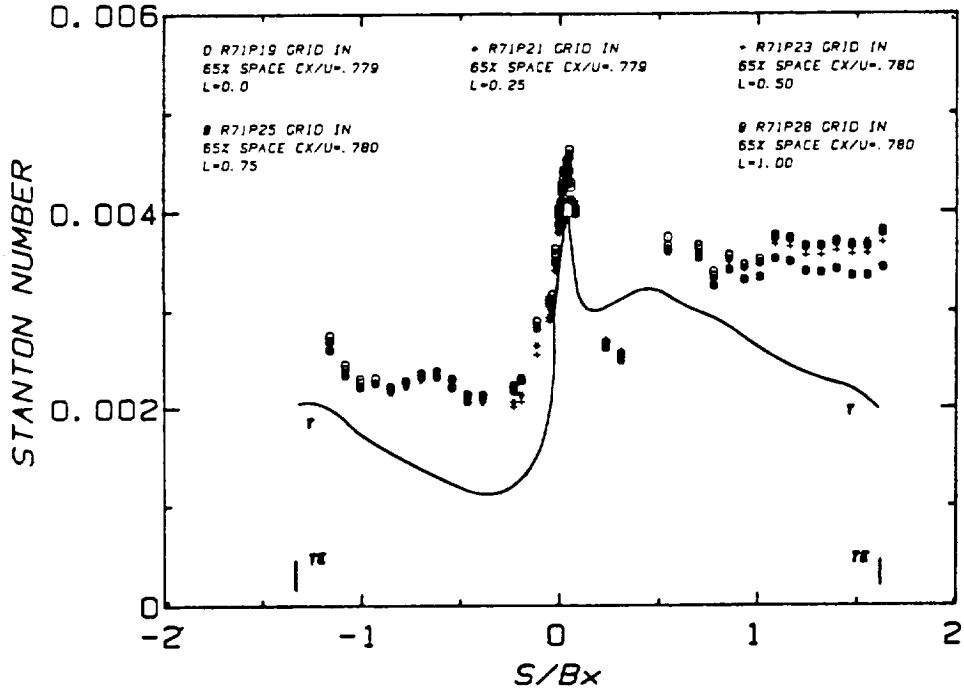

b) GRID IN

Figure 9 Effects of the Upstream Grid and the Relative Circumferential Positions of the First and Second Stators on the Second Stator Heat Transfer, 1-1/2 Stage Configuration, Design Flow Coefficient.

DATA SETS	Re_N RANGE	Re_{BX} RANGE
R66P05 R70P04 R67P02 R70P05 R67P03 R70P07 R70P02 R70P11	13280-36080	242800-642900

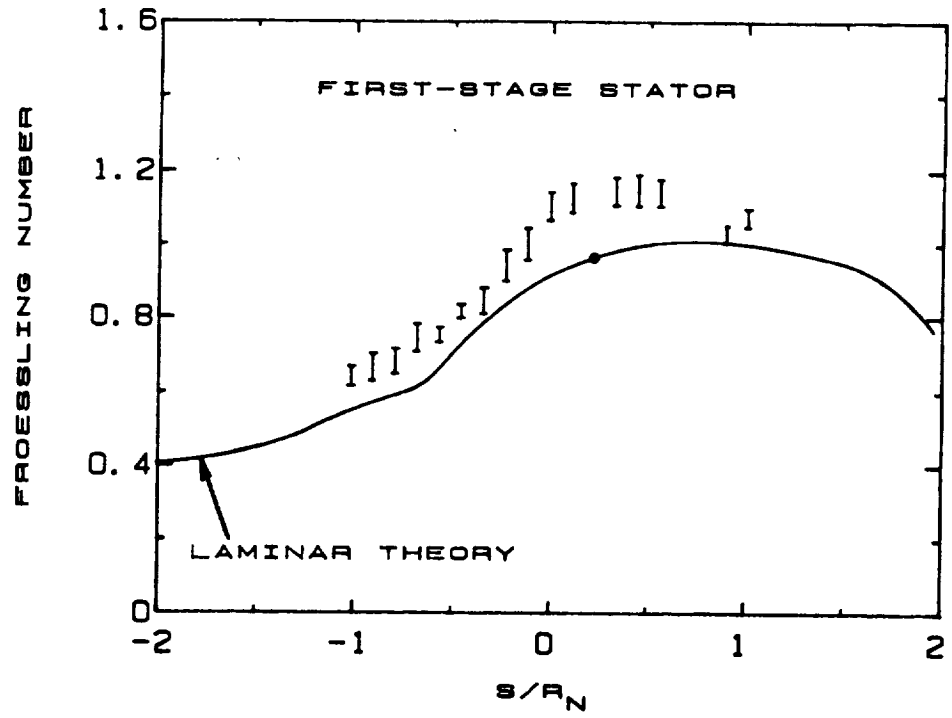

Figure 10 Measured and Predicted Heat Transfer Distributions for the Leading Edge Region of the First-Stage Stator. Data Obtained Over a Range of Reynolds Numbers With the Upstream Grid In.

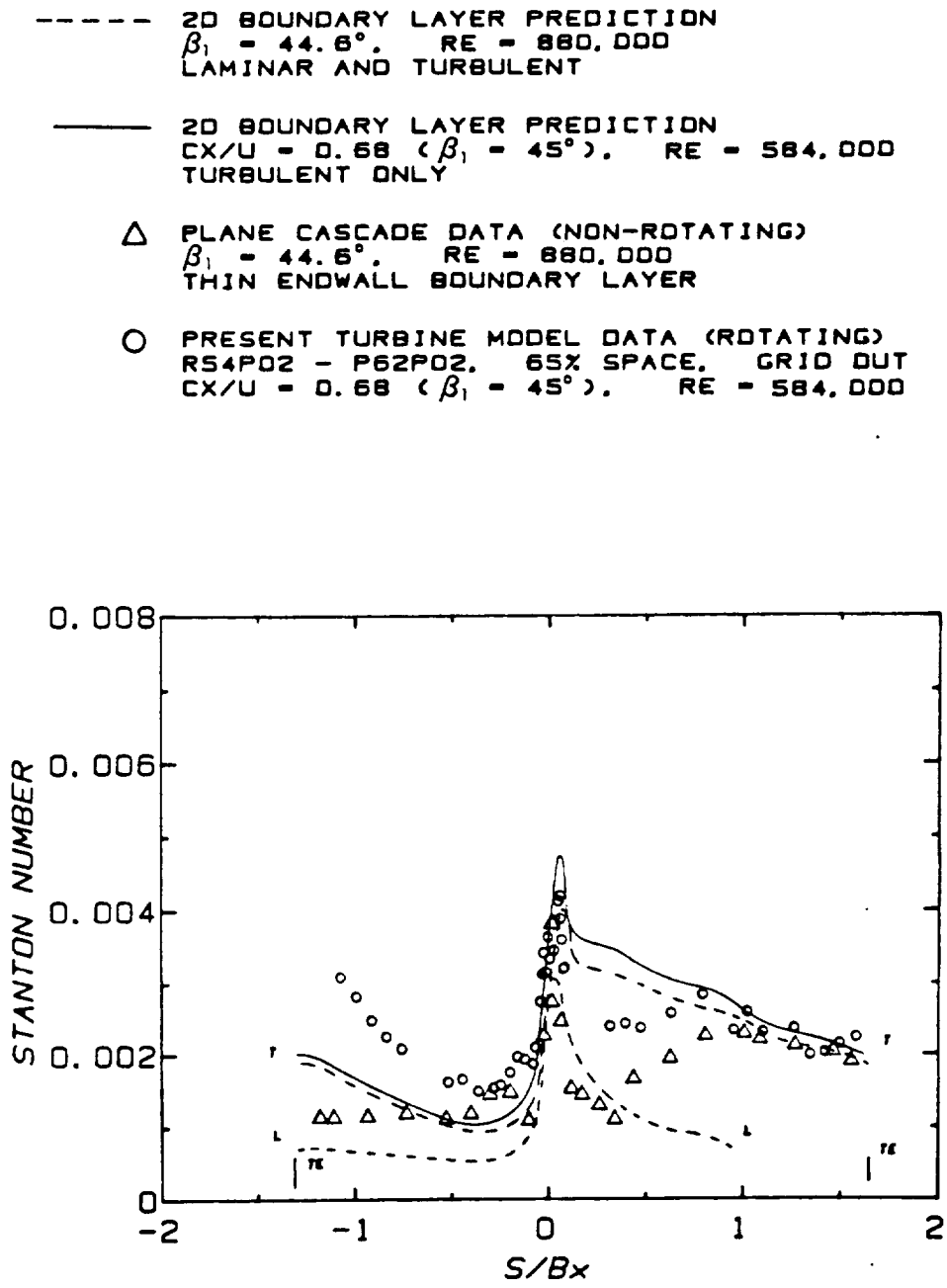

Figure 11 Comparison of Measured and Predicted Heat Transfer Distributions for the Rotor in the Present Rotating Turbine Model and the Same Airfoil Midspan Geometry Installed in a Plane Cascade (Non-Rotating).

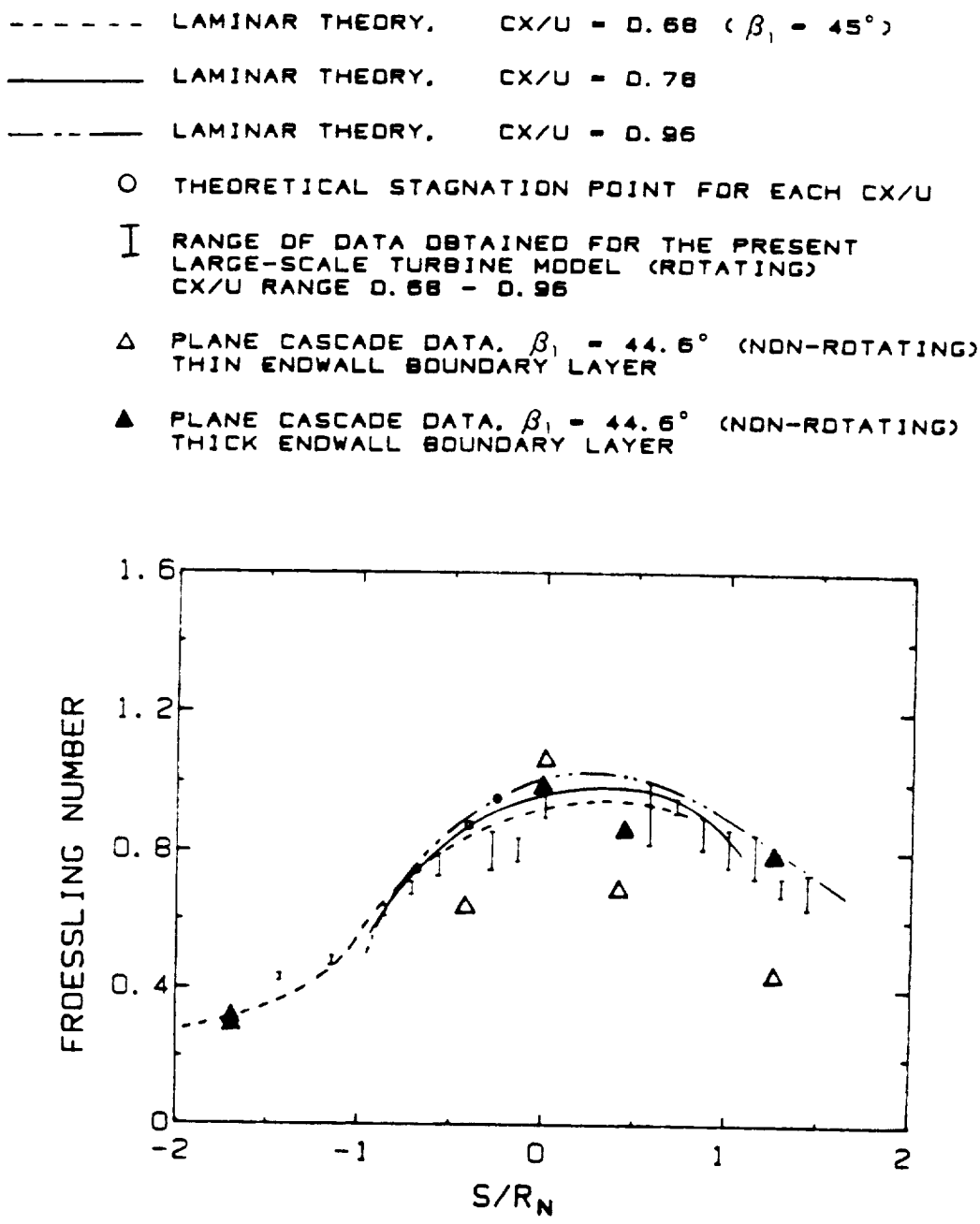

Figure 12 Comparison of Measured and Predicted Heat Transfer Distributions for the Leading Edge Region of the Rotor. Data Obtained on the Present Rotating Turbine Model and for the Same Airfoil Midspan Geometry Installed in a Plane Cascade (Non-Rotating).